



**Fermi National Accelerator Laboratory**

**FERMILAB-Conf-93/385-E**

**DØ**

# **Search for the Top Quark in the Electron-Electron and Electron-Muon Channels at DØ**

**Presented by Mirek Fatyga  
For the DØ Collaboration**

*Fermi National Accelerator Laboratory  
P.O. Box 500, Batavia, Illinois 60510*

**December 1993**

**Presented at the 9th Topical Workshop on Proton-Antiproton Collider Physics,  
Tsukuba, Japan, October 18-22, 1993**

## **Disclaimer**

*This report was prepared as an account of work sponsored by an agency of the United States Government. Neither the United States Government nor any agency thereof, nor any of their employees, makes any warranty, express or implied, or assumes any legal liability or responsibility for the accuracy, completeness, or usefulness of any information, apparatus, product, or process disclosed, or represents that its use would not infringe privately owned rights. Reference herein to any specific commercial product, process, or service by trade name, trademark, manufacturer, or otherwise, does not necessarily constitute or imply its endorsement, recommendation, or favoring by the United States Government or any agency thereof. The views and opinions of authors expressed herein do not necessarily state or reflect those of the United States Government or any agency thereof.*

# Search for the Top Quark in the Electron-Electron and Electron-Muon Channels at DØ

The DØ Collaboration  
presented by Mirek Fatyga  
*Brookhaven National Laboratory*  
*Upton, NY, 11973-5000, USA*

December 3, 1993

## Abstract

We discuss preliminary results of a search for top quarks using their decays in two di-lepton channels, with the DØ detector at Fermilab. The present analysis has been optimized to search for a top with mass near  $100 \frac{GeV}{c^2}$ , consistent with published limits. In the event sample corresponding to an integrated luminosity of  $15 \text{pb}^{-1}$  we observe two events passing all selection cuts. The number of events observed is consistent with the expected number of background events. Consequently, we do *not* claim the observation of a top decay in the present event sample. We note however, that the kinematic properties of one of the events appear to be far removed from known backgrounds. We discuss the event and show results of the mass likelihood analysis when applied to this event.

## 1 Introduction

This article gives preliminary results of a search for standard model top quark production in  $p\bar{p}$  collisions at  $\sqrt{s} = 1.8 \text{TeV}$ , using the DØ detector at the Fermilab Tevatron. For this search we have assumed, consistent with CDF's published lower mass limit[1], and standard model theoretical expectations, that the top quark is produced in quark-antiquark ( $t\bar{t}$ ) pairs, with each quark decaying 100% of the time to an on-shell  $W$  boson and a  $b$  quark. To produce a di-lepton decay, each  $W$  boson is required to decay into a lepton and a neutrino. We present results of a search in two channels, di-electron and electron-muon. The search for a muon-muon decay is in progress. The full experimental signature consists of two high  $P_T$  isolated leptons, missing transverse energy ( $E_T$ ) from both neutrinos and some jet activity in the detector. In principle, a minimum of two jets should be required to account for the production of two  $b$  quarks. A better experimental acceptance is obtained however, if one allows for a loss of one of the two jets due to the incomplete coverage of the solid angle by the DØ calorimeter. The number of jets required is determined through the optimization of a signal to background ratio. Approximate branching ratios for di-lepton channels are 2.47%

in the  $e - \mu$  channel and 1.23% in the  $e - e$  channel.

## 2 Particle Identification

This section contains brief descriptions of the methods used to identify the final state particles in the DØ detector. Additional information about the particle identification in the DØ detector can be found in other articles in these proceedings. For high  $P_T$  electron and muon identification, see Ref. [3], for jets see Ref. [4]. For a description of the DØ detector, see Refs. [3] and [5].

The electron identification algorithm is seeded by an isolated cluster of energy in the electromagnetic compartment of the calorimeter. Electron identification requirements are imposed on the longitudinal and the transverse shower shapes in the calorimeter. Longitudinally, we require that at least 90% of the cluster energy is contained in the electromagnetic compartment of the calorimeter. The transverse shower shape is analyzed on the basis of the energy deposition in the peak of the shower, which is contained in the finely segmented third layer of the electromagnetic compartment. The transverse segmentation in this layer is  $0.05 \times 0.05$  in  $\eta \times \phi$ . The longitudinal and transverse shower shape information is combined through the covariance matrix analysis[3]. In addition to the shape of the shower in the calorimeter, electrons were required to have an associated matching track in the central tracking chambers. The top analysis requires that the electron is isolated from all other energy depositions in the calorimeter. The isolation criterion is defined in Ref.[3]. For the purpose of this analysis the isolation criterion has been tightened to 10% (as opposed to 15% in the electron identification standard [3]). We imposed on electrons a cut in pseudorapidity ( $\eta$ ) of  $|\eta| < 2.5$ . The minimum transverse energy cut used in the analyses presented here was  $E_T > 20\text{GeV}$  in the  $e - e$  channel and  $E_T > 15\text{GeV}$  in the  $e - \mu$  analysis. The choice of these particular  $E_T$  thresholds was dictated by background considerations.

Muons were identified by the track in the muon spectrometer, accompanied by the deposition of at least minimum ionizing energy in the calorimeter along the path of the muon. Four track quality requirements are used to characterize a muon track: tracks are required to have a good quality of the fit in the bend and the non-bend view, and a good quality of the track projection on the reconstructed vertex in both views. The good muon track was allowed to fail at most one of the four track quality criterions. The fiducial region for the  $e - \mu$  analysis is  $|\eta| < 1.7$ , which corresponded to the acceptance edge of the wide angle muon spectrometer. High  $P_T$  isolated muons were required to be isolated from other energy in the calorimeter and to pass a minimum  $P_T$  cut of  $P_T > 15\text{GeV}$ . The momentum resolution in the muon system can be parametrized as  $\delta(\frac{1}{p}) = 0.2p \pm 0.01(\frac{\text{GeV}}{c})^{-1}$ .

Jets were reconstructed using a cone algorithm of radius 0.5 in  $\eta \times \phi$  space. The fiducial  $\eta$  range for jets was  $|\eta| < 4.0$ , which corresponded to the acceptance edge of the calorimeter. Jets had a minimum  $E_T$  cut in all of the analyses of  $E_T > 15\text{GeV}$ .

The presence of one or more neutrinos in the final state was inferred from an overall transverse energy imbalance ( $\cancel{E}_T$ ) based on all detected particles and the calorimeter energy. The specific  $\cancel{E}_T$  cut varied among the analyses. The  $e - \mu$  analysis also made use of a more restricted definition of missing  $E_T$  based on calorimeter information only (i.e. excluding

Event type	Events
$WW \rightarrow e + e + \cancel{E}_T$	0.1
$Z \rightarrow \tau\tau$	0.1
QCD (multijet, W+jets)	0.3
Total background	$0.5 \pm 0.3$

Table 1: The estimated number of background events satisfying  $e + e + \text{jets}$  selection cuts.

Event type	Events
$WW \rightarrow e + \mu + \cancel{E}_T$	0.2
$Z \rightarrow \tau\tau$	0.4
QCD (W+jets)	0.4
Total background	$1.1 \pm 0.3$

Table 2: The estimated number of background events satisfying  $\mu + e + \text{jets}$  selection cuts for various jet multiplicities.

muons). This quantity, referred to as  $\cancel{E}_T^{\text{cal}}$ , is a measure of the  $E_T$  carried by neutrinos and muons. It is a useful supplement to the direct measurement of muons because it has better resolution when the muon momentum is high and because it is insensitive to cosmic rays.

### 3 Background Processes

One may separate background processes into two categories. In the first category are irreducible physics backgrounds, which produce events with all properties of the  $t\bar{t}$  decay. All objects in such an event (leptons, neutrinos, jets) are real and originate at the interaction vertex. In the second category are instrumental backgrounds, consisting of events in which at least one of the physics objects is false, resulting from a misidentification due to experimental fluctuations.

Two leading physics backgrounds (in both decay channels) are the production of  $W$  pairs and the production of the  $Z$  boson followed by its decay into  $\tau$  leptons. The leading source of instrumental backgrounds in both channels is a production of the  $W$  boson accompanied by jets, with one of the jets producing a fake electron signal due to instrumental fluctuations. An additional background in the  $e - e$  channel is caused by  $QCD$  multi-jet events with *two* jets fluctuating into fake electron signals and the missing transverse energy fluctuating into a fake neutrino signal, the latter due to a mismeasurement of jet energies.

The expected background yields in the full event sample, for both channels, are listed in Tables 1 and 2.

### 4 Analysis of $t\bar{t} \rightarrow \mu + e + \text{jets}$ .

This section describes event selection for the  $\mu + e + \text{jets}$  final state.

Three independent triggers were used to record these data:

- One electron with  $E_T > 7\text{GeV}$ , and one muon with  $P_T > 5\text{GeV}$ .

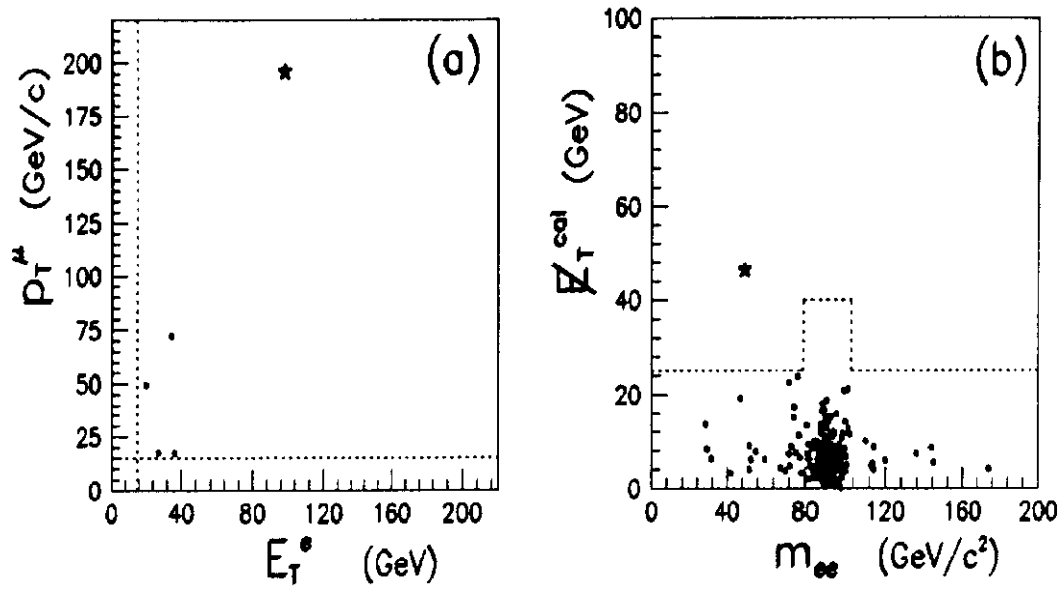


Figure 1: Scatter plots illustrating the event selection. The  $\mu + e + \text{jets}$  channel in plot (a) and the  $e + e + \text{jets}$  channel in plot (b). Events passing all selection cuts are marked by a star.

- One electron with  $E_T > 12\text{GeV}$ ,  $\cancel{E}_T > 20\text{GeV}$ , one jet with  $E_T > 16\text{GeV}$ .
- One muon with  $P_T > 14\text{GeV}$ ,  $\cancel{E}_T > 12\text{GeV}$ , one jet with  $E_T > 15\text{GeV}$ .

The data sample used for this analysis had an integrated luminosity of  $15.2 \pm 1.8\text{pb}^{-1}$ . The offline event selection begins with a requirement of two isolated leptons (one electron, one muon), both with transverse energy (momentum) greater than  $15\text{GeV}$ . 27 events remain after the initial selection.

The second criterion requires that the missing transverse energy measured in the calorimeter *only* is greater than  $20\text{GeV}$ . 15 events remain after this cut.

The third criterion requires that the missing transverse energy measured in the calorimeter and corrected for the muon momentum is greater than  $20\text{GeV}$ . 8 events remain after this cut.

The fourth criterion requires a minimum separation in the  $(\eta \times \phi)$  space between a muon and an electron ( $R > 0.25$ ). The purpose of this criterion is to reject events due to the colinear muon bremsstrahlung. 5 events remain after this cut.

The fifth and final criterion requires one jet with the transverse energy greater than  $15\text{GeV}$ . 1 event remains after this cut.

The process of event selection is illustrated by Fig.1a. The transverse momentum of a muon is plotted against the transverse energy of an electron. The plot shows data in the  $\mu + e + \text{jets}$  channel after the first four selection cuts (prior to a jet requirement). The event passing the jet selection cut is located at the top of the scatter plot. Properties of the sole event passing all cuts are listed in Table 3.

Object	Observable	Value
electron	$E_T$	$98.8 \pm 1.6 \text{ GeV}$
muon	$P_T$	$195 \text{ GeV}$
muon (error)	$P_T(\text{min})$	$P_t > 40 \text{ GeV at } 95\% \text{ CL}$
jet 1	$E_T$	$26.1 \pm 4.1 \text{ GeV}$
jet 2	$E_T$	$23. \pm 2.4 \text{ GeV}$
jet 3	$E_T$	$7.9 \pm 1.2 \text{ GeV}$
neutrinos	$\cancel{E}_T$	$101 \text{ GeV}$
neutrinos (error)	$\cancel{E}_T(\text{min})$	$\cancel{E}_T > 54 \text{ GeV at } 95\% \text{ CL}$

Table 3: Properties of the  $e - \mu$  event passing all selection cuts.

## 5 Analysis of $t\bar{t} \rightarrow e + e + \text{jets}$

This section describes triggers and the offline event selection for the  $e + e + \text{jets}$  final state. We discuss numerical estimates of background yields and the kinematic properties of the single event which remains after all selection cuts.

Three independent triggers were used to record these data:

- One electron with  $E_T > 20 \text{ GeV}$ , and  $\cancel{E}_T^{\text{cal}} > 20 \text{ GeV}$ .
- Two electrons with  $E_T > 20 \text{ GeV}$ .
- One electron with  $E_T > 15 \text{ GeV}$ ,  $\cancel{E}_T^{\text{cal}} > 20 \text{ GeV}$ , one jet with  $E_T > 16 \text{ GeV}$ .

The data sample used for this analysis had an integrated luminosity of  $15.2 \pm 1.8 \text{ pb}^{-1}$ . The offline analysis begins with a selection of two isolated electrons, each with  $E_T > 20 \text{ GeV}$ . Events selected by this criterion are dominated by di-electron pairs due to decays of the  $Z$  boson. 904 events remain after this cut.

The second criterion requires that the absolute value of a difference between the invariant mass of a pair in an event and the  $Z$  boson mass is greater than  $12 \text{ GeV}$ . To maximize the acceptance, an exclusion to this cut is provided when the missing transverse energy in the event is greater than  $40 \text{ GeV}$ . Both elements of the second selection criterion are based on the analysis of Monte Carlo  $Z$  decays as well as an analysis of data sample of  $Z$  bosons which are not accompanied by jets. 146 events remain after this cut.

The third criterion requires the missing transverse energy in the event  $\cancel{E}_T > 25 \text{ GeV}$ . 4 events remain after this cut.

The fourth criterion requires one jet with the transverse energy  $E_T > 15 \text{ GeV}$ .

One event passes all the selection criteria. The selection process is illustrated by the Fig.1b. There, we show scatter plots of the di-electron invariant mass plotted against the missing transverse energy in an event. The data sample shown in this plot are events which re-

Object	Observable	Value
electron 1	$E_T$	$36 \pm 1 \text{ GeV}$
electron 2	$E_T$	$29 \pm 1 \text{ GeV}$
di-electron pair	$M_{ee}$	$49 \pm 1 \text{ GeV}$
jet 1	$E_T$	$63 \pm 11 \text{ GeV}$
jet 2	$E_T$	$19 \pm 3 \text{ GeV}$
neutrinos	$\cancel{E}_T$	$47 \pm 11 \text{ GeV}$

Table 4: Properties of the  $e - e$  event passing all selection cuts.

Top mass $\frac{\text{GeV}}{c^2}$	$\mu + e + \text{jets}$	$e + e + \text{jets}$
100	6.2	2.9
120	2.5	1.4
140	1.2	0.6
160	0.6	0.3
180	0.3	0.2

Table 5: Expected number of events in the full event sample (integrated luminosity of  $15.2 \text{ pb}^{-1}$ )

main after two offline selection requirements: a requirement of two isolated leptons and a requirement of at least one jet with  $E_t > 15 \text{ GeV}$ . A dotted line shows the  $\cancel{E}_T$  cut with an indentation for the  $Z$  mass cut. The data sample is clearly dominated by products of a decay of the  $Z$  boson. The properties of the one  $e - e$  event passing all selection cuts are listed in Table 4.

## 6 Acceptances and Expected Signal Event Rates.

The expected cross section for  $t\bar{t}$  production is calculated on the basis of the NNLO (Next-to-Next-to-Leading-Order) calculation by Laenen et al.[6] Cross sections are multiplied by efficiencies derived from Monte Carlo simulations.  $t\bar{t}$  pairs are generated by the ISAJET Monte Carlo, and DØGeant is used to simulate the detector response. Efficiencies in both channels depend on the mass of the top, but the dependence is a weak one with the present set of cuts. As mentioned earlier, the present set of cuts has been optimized to give one maximum possible sensitivity at relatively small masses of the top (around  $100 \frac{\text{GeV}}{c^2}$ ). Stronger mass dependence would be observed with a set of harder cuts. Expected event yields for both channels, as a function of the top mass, are shown in Table 5. The systematic uncertainty on efficiencies is 28% in the  $\mu + e + \text{jets}$  channel and 15% in the  $e + e + \text{jets}$  channel.



## 7 Mass Analysis of the $\mu + e + \text{jets}$ Event.

The single  $\mu + e + \text{jets}$  event which passes top selection cuts has kinematic properties that are unlikely for typical background event. This statement can be illustrated by the following: Suppose that we change our off-line selection cuts (in the  $\mu + e + \text{jets}$  channel) by doubling their numerical values, so as to require two leptons with  $P_T > 30\text{GeV}$ , the  $\cancel{E}_T$  above  $40\text{GeV}$  and at least two jets with  $E_t > 15\text{GeV}$ . After repeating background calculations, one finds that the expected number of events has been reduced by a factor of 10 (to 0.1 events). The expected number of signal events in the full sample is reduced by approximately a factor of three for the top quark with the mass above  $120 \frac{\text{GeV}}{c^2}$ . The  $\mu + e + \text{jets}$  event passes these cuts. Clearly, this event is located in the region of phase space where the signal to background ratio is much more favorable than the one presented in the first part of this paper. The only processes that still contribute to the background are  $WW \rightarrow e\mu$  and  $Z \rightarrow \tau\tau \rightarrow e\mu$ . Hence, we have performed an analysis of kinematic properties of the  $e\mu$  event under an assumption that the event has indeed been produced as a result of a decay of the  $t\bar{t}$  pair. *We stress, that results of this analysis should not be misconstrued as a proof of top discovery. We simply seek to convince ourselves that the event is kinematically consistent with the hypothesis of top production and decay, with a reasonable value of the top mass. It is not possible to claim discovery of the top quark on the basis of a single event, no matter how striking the event might be.*

Mass analysis of the type described here has been proposed independently by Kondo [7] and Dalitz and Goldstein[8]. The full kinematics of an  $e\mu$  final state can be described by eighteen independent kinematic variables (three variables for each of the six objects in the final state). Assuming some mass of the top quark  $M_t$ , there are four kinematic constraints: two mass constraints on  $W$  bosons and two mass constraints on top quarks. There are fourteen independent observables (lepton momenta, jet energies and the  $\cancel{E}_T$ ). Hence, for an assumed mass of the top quark, one can solve a set of kinematic equations, completely determining the kinematics of the top pair. For every assumed mass of the top, one obtains zero, two or four solutions. The analysis is repeated on an ensemble of simulated events obtained by a Monte Carlo smearing of measured kinematic variables. A smearing procedure for each variable is designed to simulate the appropriate instrumental resolution. Furthermore, we have to deal with ambiguities in assigning jet identities. We need to identify b-jets and pair them correctly with leptons. Since the  $e\mu$  event has *three* jets, one also has to deal with complications due to the initial and the final state radiation. We assign jet identities in a probabilistic fashion, thus further expanding the space of solutions. If all the solutions were assigned the same weight, a mass peak does not result since we can get solutions from very heavy top quarks that are consistent with the observed 4-momenta. In order to get mass information out of this analysis, one needs to weight each solution with the probability that it is due to the production and decay of the top quark. This has the effect of damping down high mass solutions, since they are rendered unlikely to be produced at Tevatron energies by parton fusion. Because of the sensitivity of the mass determination to the weighting scheme, we have experimented with three different schemes. In Method I,[9], the production weight is given by

$$WT = \frac{1}{\sigma_{vis}} \frac{d\sigma}{d(LIPS)}$$

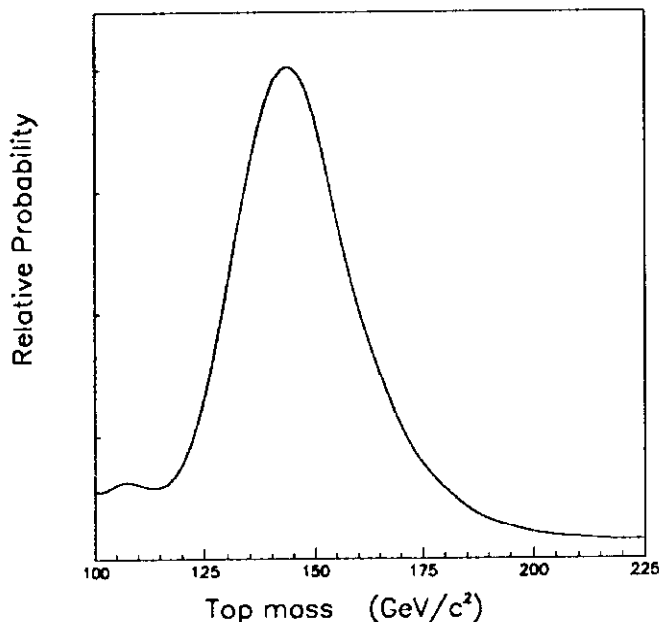


Figure 2: Results of the Mass Analysis procedure using Methods I and II.

where  $\sigma_{vis}$  is the cross section observed in the detector at the top mass in question and  $d(LIPS)$  is the Lorentz Invariant Phase Space volume element for  $t\bar{t}$  production represented by the solution. This scheme has implicit in it a product of the structure functions appropriate to parton fusion. The weight is normalized to the visible cross section so that low mass solutions are not unfairly favored. The probability of observing the decay products from  $t\bar{t}$  decay are estimated as per [8] and is common to all weighting schemes. Method II,[10], uses a slightly different variant of the above

$$WT = \frac{1}{\sigma_{vis}} \frac{d\sigma}{d(\text{observed variables})}$$

where the observed variables are taken to be boost invariant quantities derived from the observed 4-momenta. To account for effects of the initial state radiation, one computes the transverse energy  $k_T$  of the  $t\bar{t}$  pair for a given jet assignment. One weights the event by the probability of observing that  $k_T$  for the  $t\bar{t}$  system, for the jet combination in question, based on a study of Isajet generated events. Final state radiation effects are also estimated by parametrizing the probability of secondary jet emission in terms of the observed jet variables again using Isajet events.

The results obtained by methods I and II are sufficiently close to each other that we have combined them into one figure 2.

Method III follows the original Dalitz-Goldstein method more closely. Here the weight used is

$$WT = F(x_1)F(x_2)$$

which is a product of the structure functions. The resulting likelihood curve for the leading jet combination (assuming that two leading jets are b-jets) is shown in figure 3. One can study the validity of these methods using Monte Carlo events generated for various discrete top masses. The value of the mass at the peak of the likelihood function on average does

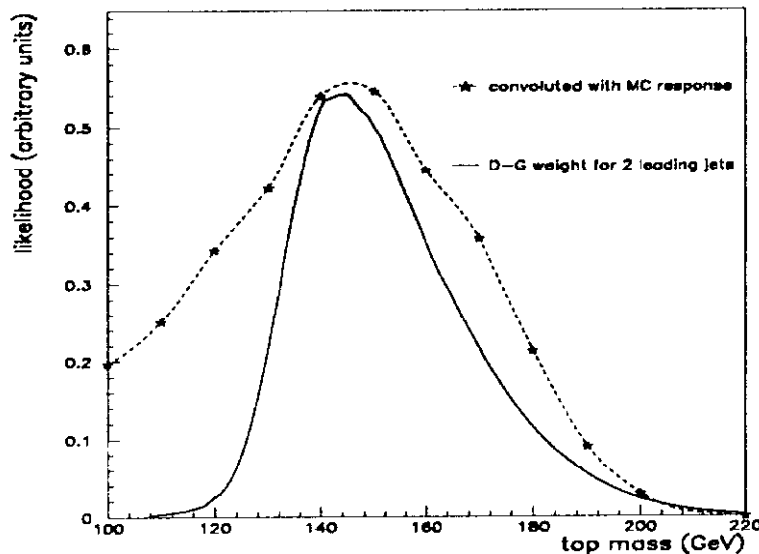


Figure 3: Results of the Mass Analysis procedure using Method III.

represent a good measure of the generated mass. The dashed line in figure 3 represents the relative probability of observing an event for which the likelihood function peaks at  $145 \frac{\text{GeV}}{c^2}$ . One should emphasize that each individual event likelihood distribution contains more information than just its peak value. The width in mass of the distribution reflects the kinematics of the event. The unfolding scheme described here only uses the peak information and as such gives a broader likelihood curve than the event specific likelihood curve. In summary, all three methods of Mass Analysis lead to similar results. The  $\mu + e + \text{jets}$  event in our sample is kinematically consistent with the top decay. The likelihood distribution plotted with respect to the top mass peaks at  $142 \frac{\text{GeV}}{c^2}$ .

## 8 Conclusions

In conclusion, we searched for the production of Standard Model  $t\bar{t}$  pairs in two di-lepton channels,  $e + e + \text{jets}$  and  $\mu + e + \text{jets}$ . We found two events passing all selection cuts, one in each channel. The number of events observed is consistent with expected backgrounds. Based on the present data sample, we conclude that the decay of the top quark has *not* been observed in di-lepton channels. The lower limit on the mass of the top quark, derived by combining the results of this analysis and the search for top decays in other channels is presented in Ref.[11]

## References

- [1] F. Abe *et al.*, Phys Rev **D45**, 3921 (1992).

- [2] W. T. Giele *et al.*, Fermilab-Pub-92/230-T (1992); W. T. Giele *et al.*, Fermilab-Conf-92/213-T (1992).
- [3] N. Graf, "Production of W and Z Bosons at DØ" these proceedings.
- [4] H. Weerts, "Studies of Jet Production in the DØ Detector," these proceedings.
- [5] S. Abachi *et al.*, Submitted to Nucl. Inst. and Methods in Phys. Res. and Fermilab-Pub-93/179 (July 1993).
- [6] E. Laenen, J. Smith, W. van Neerven, Nuclear Physics, **B369**, 543 (1992); E. Laenen, Fermilab-Pub-93/155-T (1993); E. Laenen, J. Smith, W. van Neerven, Fermilab-Pub-93/270-T (1993). For the top yield we used the central value estimate while for the mass limit calculation we used the lower limit estimate.
- [7] K.Kondo, T.Chikamatsu and S.Kim, Journal of the Phys. Soc. of Japan, **62**, 1177 (1993).
- [8] R.H.Dalitz and G.R.Goldstein, Phys.Lett. **B287**, 225 (1992).
- [9] R.Raja DØ Note 1978, Unpublished.
- [10] DØ collaboration, M.Strovink, "Proceedings of the International Europhysics Conference on High Energy Physics", Marseille (1993), eds. J.Carr and M.Perrottet.
- [11] H. Greenlee, "Searches for the Top Quark in the Single Lepton + Jets Channels at DØ" these proceedings.